https://doi.org/10.5194/amt-2022-26
Preprint. Discussion started: 26 January 2022

Atmospheric Measurement Techniques Discussions

Intercomparison of wind observations from ESA's satellite mission Aeolus, ERA5 reanalysis and radiosonde over China

Boming Liu[1], Jianping Guo[2*], Wei Gong[1*], Yong Zhang[3], Lijuan Shi[3], Yingying Ma[1], Jian Li[2], Xiaoran Guo[2], Ad Stoffelen[4], Gerrit de Leeuw[4], and Xiaofeng Xu[5]

[1] State Key Laboratory of Information Engineering in Surveying, Mapping and Remote Sensing (LIESMARS), Wuhan University, Wuhan, China
[2] The State Key Laboratory of Severe Weather, Chinese Academy of Meteorological Sciences, Beijing 100081, China
[3] Meteorological observation Centre, Chinese Meteorological Administration, Beijing 100081, China
[4] The Royal Netherlands Meteorological Institute (KNMI), 3730 AE De Bilt, The Netherlands
[5] Chinese Meteorological Administration, Beijing 100081, China

Correspondence to: Dr./Prof. Jianping Guo (Email: jpguocams@gmail.com) and Wei Gong (Email: weigong@whu.edu.cn)

Abstract. The European Space Agency (ESA) Earth Explorer Atmospheric Dynamics Mission Aeolus is the first satellite mission providing wind profile information on a global scale, and its wind products have been released on 12 May 2020. Here we verify and intercompare the wind observations from ESA's satellite mission Aeolus and the European Centre for Medium-Range Weather Forecasts (ECMWF) fifth generation atmospheric reanalyses (ERA5) with radiosonde (RS) observations over China, to allow a fitting application of Aeolus winds. Aeolus provides wind observations in aerosol-free (referred to as Rayleigh-clear winds) and cloudy atmospheres (Mie-cloudy winds). In terms of Aeolus and RS winds, the correlation coefficient (R) and mean difference of Rayleigh-clear (Mie-cloudy) vs RS winds are 0.94 (0.97) and −0.24±7.01 (0.18±4.42) m/s, respectively. The vertical profiles of wind speed differences between Aeolus and RS winds are similar to each other during ascending and descending orbits. The comparison of ECMWF winds relative to Aeolus winds provides the R and mean difference of Rayleigh-clear (Mie-cloudy) winds, which are 0.95 (0.97) and −0.16±6.78 (−0.21±3.91) m/s, respectively. The Rayleigh-clear and Mie-cloudy winds are very consistent with the ECMWF winds, likely due to the assimilation of Aeolus wind observations into the ECMWF analysis. Moreover, we find that among the results of comparing Aeolus with RS and

https://doi.org/10.5194/amt-2022-26
Preprint. Discussion started: 26 January 2022


Atmospheric Measurement Techniques Discussions

ECMWF winds, a small difference between Rayleigh-clear winds relative to RS winds is appeared in the height range of 2−3 km during descending orbits. This result may be due to the high vertical velocity during the descending orbits. The mean differences between Rayleigh-clear (Mie-cloudy) winds and RS winds during the ascending and descending orbit phase are −0.07 ±0.69 (−0.72 ±1.48) and 0.3 ±1.25 (0.1 ±1.32) m/s. These small deviations indicate that the performance of Aeolus wind products may be unaffected by the orbit phase or HLOS wind conditions. In addition, the R and mean difference between ERA5 and RS zonal wind components are 0.97 and −0.46 ±3.12 m/s, respectively. Overall, the Aeolus winds over China are similar to the RS and ECMWF winds. The findings give us sufficient confidence and information to apply Aeolus wind products in numerical weather prediction in China and in climate change research.

1 Introduction

Atmospheric three-dimensional wind fields play a key role for the prediction of extreme events (Pu et al., 2010; Guo et al., 2018; Stettner et al., 2019), a better understanding of air pollution dispersion (Liu et al., 2018; Yang et al., 2019; Shi et al., 2020; Su et al., 2020; Zhang et al., 2020) and complex aerosol-cloud-precipitation interactions (Koren et al., 2005; Fan et al., 2009; Li et al., 2011; Guo et al., 2017; Liu et al., 2020a). Moreover, assimilating atmospheric wind observations into numerical weather prediction models is of great significance for better predicting surface wind speed and assessing the trend of wind energy changes (Benjamin et al., 2004; Constantinescu et al., 2009; Simonin et al., 2014). Therefore, continuous global wind profile observations are desperately needed for advancing our knowledge of atmospheric dynamics as well as for improving the accuracy of numerical weather prediction (Houchi et al., 2010; Albertema et al., 2019; Stoffelen et al., 2005; 2020).

The European Space Agency (ESA) Earth Explorer Atmospheric Dynamics Mission Aeolus, launched on 22 August 2018, is the first satellite mission designed to acquire atmospheric wind profiles on a global scale by employing a Doppler Wind Lidar payload, called Atmospheric LAser Doppler

https://doi.org/10.5194/amt-2022-26
Preprint. Discussion started: 26 January 2022


Atmospheric Measurement Techniques Discussions

INstrument (ALADIN, Reitebuch, 2012; ESA, 2008; Stoffelen et al., 2005). The flight altitude and repeat cycle of the Aeolus satellite are about 320 km and 7days, respectively (Witschas et al., 2020). It provides measurements of the wind vector component along the instrument's line-of-sight from the ground up to 30 km altitude (Rennie et al., 2020). The Aeolus wind products have been released on 12 May 2020 (https://earth.esa.int/eogateway/news/aeolus-data-now-publicly-available, last access: 13-01-2021), the vertical resolution is 0.25 to 2 km, while the wind accuracy is approximately 2 to 4 m/s, depending on the altitude (Tan et al., 2017; Guo et al., 2020). The most unique products are Aeolus L2B wind products, which include the geo-located and consolidated horizontal line-of-sight (HLOS) wind observations with actual atmospheric correction and bias corrections applied. It provides scientific wind products for public users, which contain the Rayleigh-clear and Mie-cloudy winds (Tan et al., 2008). The Rayleigh-clear and Mie-cloudy winds refer to wind observations in an aerosol-free or a cloudy atmosphere, respectively (Witschas et al., 2020). The European Centre for Medium-Range Weather Forecasts (ECMWF) started to assimilate Aeolus data in their operational forecasts as of January 2020, using an internal bias correction based on their model winds (https://earth.esa.int/eogateway/news/aeolus-winds-now-in-daily-weather-forecasts, last access: 15-01-2021).

To date, the Aeolus team and related researchers across the world have carried out a series of verification and comparison work on the Aeolus wind products (Marksteiner et al., 2018; Rennie et al., 2018; Kanitz et al., 2020). Rennie and Isaksen (2020) conducted the first validation of the Aeolus Level 2B product against the ECMWF numerical weather prediction model, which played a crucial role in the Aeolus characterization. At the same time, Witschas et al. (2020) carried out comprehensive validation of Aeolus measurements against airborne Doppler wind lidar observations. The mean biases of line-of-sight wind speeds for the airborne Doppler wind lidar and the Aeolus against the ECMWF model were −0.9 m/s and +1.6 m/s, respectively (Lux et al., 2020). Moreover, the Aeolus wind products have been compared with RS data above the Atlantic Ocean, from which the systematic and

https://doi.org/10.5194/amt-2022-26
Preprint. Discussion started: 26 January 2022


Atmospheric Measurement Techniques Discussions

statistical errors of the Rayleigh (Mie) winds were found less than 1.5 (1.0) and 3.3 (1.0) m/s, respectively (Baars et al., 2020). Martin et al. (2020) compared the Aeolus winds with radiosonde (RS) observations and two numerical weather prediction model equivalents, confirming that the performance of Aeolus wind products can be easily affected by satellite flight direction, seasonal differences and geographic changes. In addition, Guo et al. (2020) evaluated the performance of Aeolus wind products over China by comparing with data from the ground-based radar wind profiler network of China. The above-mentioned verification exercises have deepened our understanding of the global Aeolus wind products and led to improvements in Aeolus products. However, since the radar wind profiler network of China is mainly distributed in eastern China, the performance of Aeolus wind products over central and western parts of China has not been specifically investigated. To fill this gap, it is worthwhile to further verify the performance of Aeolus wind products in China using the China's RS observation network. This network comprises 120 RS sites homogeneously distributed across mainland China and provides atmospheric soundings of winds (Guo et al., 2016; 2019). The use of these data, together with ERA-5 reanalysis data, provides a unique opportunity to deepen our understanding of the performance of Aeolus wind products over all mainland China.

To this end, a comparison is made of Aeolus, ERA5 and RS wind data over China. First, we analysed the correlations and differences between each of the three data sets, and then spatially investigated their wind component differences vertically and horizontally. The paper is organized as follows. First, the three types of wind data such as Aeolus, ERA5 and RS are briefly described (Section 2.1-2.3); the data matching principles are represented in detail in Section 2.4; and the statistical approach is addressed in Section 2.5. Section 3 presents a comprehensive comparison of Aeolus, ERA5 and RS wind observations. Finally, the main findings are summarized in Section 4.

https://doi.org/10.5194/amt-2022-26
Preprint. Discussion started: 26 January 2022


Atmospheric Measurement Techniques Discussions

2 Data and methods

2.1 Aeolus wind data

Aeolus is the first ever satellite designed to directly observe atmospheric wind profiles on a global scale (ESA, 2008; 2016). The ground tracks of Aeolus over China are shown in Fig. 1. The red and blue lines represent the ascending and descending ground tracks, respectively. After the Aeolus data is disclosed, there have been three data processor releases: baseline 12 (26 May 2021 – present), baseline 11 (8 Oct 2020 – 26 May 2021) and baseline 10 (20 Apr – 8 Oct 2020). In this study, the Aeolus Level 2B (L2B) wind products from 20 April 2020 to 30 September 2020 are collected for comparison. Therefore, the L2B processor release during this period should be the baseline 10. In addition, the generation of AUX_TEL files have changed from once to twice per day (based on the previous 24 hours of data) since August 10, 2020. This file is used to perform the telescope temperature bias correction. It should give only a small quality improvement for Aeolus wind products. Therefore, we think that there were no dramatic changes in the Aeolus winds from 20 April 2020 to 30 September 2020. The L2B products contain the HLOS winds for the Rayleigh-clear winds and Mie-cloudy winds. The quality of the Aeolus wind data is indicated by validity flags (0=invalid and 1=valid) and estimated errors. The estimated error is the theoretical value calculated based on the signal intensity as well as the temperature and pressure sensitivity of the Rayleigh channel response (Dabas et al., 2008), which can be used as data filtering threshold (discussed in section 2.4). In addition, the orbit of Aeolus includes the ascending (HLOS points east) at 00:00 UTC and descending (HLOS points west) orbits at 12:00 UTC. More detailed descriptions of Aeolus wind products are provided in previous studies (Reitebuch et al., 2012; ESA, 2016; Rennie et al., 2018).

https://doi.org/10.5194/amt-2022-26
Preprint. Discussion started: 26 January 2022


Atmospheric Measurement Techniques Discussions

2.2 Radiosonde wind data

The L-band RS is a new-generation sounding system that can provide fine-resolution profiles of atmospheric parameters (Guo et al., 2016). Its principle is to carry the radiosonde to high altitude through balloons to measure meteorological parameters such as temperature, pressure, humidity, wind direction and wind speed (Liu et al., 2019). Moreover, it also records the sampling time, altitude and geographic coordinates of each sampling point. The RS in China are launched twice per day at around 0000 and 1200 UTC (Zhang et al., 2020). The spatial distribution of the RS stations used in this study is shown in Fig. 1, indicated by the yellow dots. The green line approximates 90 E, which is the approximate position of Aeolus at 12:00 and 0:00 UTC. Note that at the launch times, RS in eastern China are taken about 2.5 hours after the Aeolus overpass time. This is, if at all, eastern RS will mostly match with later Aeolus tracks slightly to the west of the RS station. In this study, the RS wind data over China from 20 April 2020 to 30 September 2020 were collected for comparison.

2.3 ERA5 wind data

The ECMWF produces global numerical weather predictions for Member and Co-operating States and reanalysis data for the broader community (Hoffmann et al., 2019; Belmonte et al., 2019). The fifth generation ECMWF atmospheric reanalysis system (ERA-5) provides hourly wind fields on a 0.25 x 0.25-degree latitude/longitude grid (Hersbach et al., 2020). The zonal, u, and meridional, v, component of wind can be downloaded from https://cds.climate.copernicus.eu (last access: 13-01-2021), and the speed and direction of the horizontal wind can be calculated from the u and v component of wind (Liu et al., 2020b). The ERA5 data over China from 20 April 2020 to 30 September 2020 were downloaded for the comparison with RS data. Note that the ERA5 data has a total of 28 layers in the height range of 0–20 km, which can be used to compare with L-band RS data. However, it is not appropriate to use the value of a certain layer to match the corresponding Aeolus bin value. Therefore, following the

https://doi.org/10.5194/amt-2022-26
Preprint. Discussion started: 26 January 2022


Atmospheric Measurement Techniques Discussions

study of Lux et al. (2020), the operational ECMWF wind data from the Aeolus Level 2C (L2C) wind product are obtained to compared with Aeolus winds.

The Aeolus L2C wind product contains the wind fields from the ECMWF operational prediction model assisted by Aeolus. It provides the corresponding HLOS wind of the ECMWF wind vector for each Aeolus bin, which can be used to compare with the Aeolus HLOS winds. The L2C wind product adds two assimilation data modules on the basis of the L2B wind product: "L2C Mie Assimilation Product Confidence Data" and "L2C Rayleigh Assimilation Product Confidence Data". These two data modules are generated by the ECMWF model that has assimilated the Aeolus observation data. It contains reference information such as the observation error, background error and data assimilation quality flags, among others. The observation operator and expectations of 4D-var data assimilation are described in TN file (ECMWF TN 864, https://www.ecmwf.int/file/288329/download?token=y9cKewWP). Here, the analysed wind data from the L2C product has been utilized to directly compare with L2B wind data. The Aeolus L2C wind product is first published on 9 July 2020. Therefore, the Aeolus L2C products from 9 July 2020 to 30 September 2020 are also collected to provide the ECMWF HLOS winds.

In addition, the difference between the ERA5 and ECMWF wind data is likely caused by the fact that the ERA5 dataset is entirely independent of the Aeolus winds (https://confluence.ecmwf.int/display/CKB/ERA5%3A+data+documentation#ERA5:datadocumentation-Observations: last access: 15-01-2021), but the ECMWF winds are a compromise between assimilated Aeolus winds and the ECMWF short-range forecast (background) (https://earth.esa.int/eogateway/news/aeolus-winds-now-in-daily-weather-forecasts: last access: 15-01-2021). Although the ERA5 model is not identical to the ECMWF model used in operation, its upper air characteristics are very similar, since ECMWF uses a recent model cycle for ERA5, but runs it at a slightly lower resolution than that in operation. It should also be noted that the Chinese RS data at standard or significant levels have been assimilated in both ECMWF and ERA5 models.

https://doi.org/10.5194/amt-2022-26
Preprint. Discussion started: 26 January 2022


Atmospheric Measurement Techniques Discussions

2.4 Data matching procedures

Due to the quite different spatial-temporal resolutions and sampling of Aeolus, RS and ERA5 data, data matching procedures have to be defined before performing comparison analysis. The corresponding flowchart is presented in Fig. 2, and its detailed procedures are presented below.

2.4.1 Aeolus and RS data

Both RS and Aeolus data have been collected for the period from 20 April 2020 to 30 September 2020. The RS winds firstly should be converted to Aeolus vertical bin. The RS wind vector in each bin is projected onto the Aeolus HLOS wind using the following equation (Witschas et al., 2020):

$$v_{RS_{HLOS}} = \cos(\psi_{Aeolus} - WD_{RS}) \cdot WS_{RS} \quad (1)$$

where ψ_{Aeolus} represents the Aeolus azimuth angle; WS_{RS} and WD_{RS} are the RS wind speed and direction, respectively. Moreover, for the Aeolus bins, the height interval of each bin should be covered by RS measurements, and the average of $v_{RS_{HLOS}}$ in each Aeolus vertical bin are taken in attempt to compare with the corresponding Aeolus HLOS winds.

Next, for Aeolus winds, the Aeolus official documentation pointed out that the validity flag and estimated errors should be used to conduct quality control (Dabas et al., 2008; Tan et al., 2017). A sensitivity analysis on the estimated errors can be seen in Fig. S1. The difference between Mie-cloudy (Rayleigh-clear) wind and RS wind is large when the estimated error is larger than 6 (10) m/s. Therefore, following previous studies (Guo et al., 2020; Witschas et al., 2020), the Aeolus wind data are accepted only when the validity flag equals 1 and the estimated errors for wind are, respectively, less than 7 and 5 m/s for Rayleigh and Mie channels.

Finally, we pose constraints on the time and geographical matches before comparison. Specifically, the time difference between the RS and Aeolus wind profiles should be minimum. Due to the fact that

https://doi.org/10.5194/amt-2022-26
Preprint. Discussion started: 26 January 2022


Atmospheric Measurement Techniques Discussions

there are only two RS wind profiles (i.e., at 00:00 and 12:00 UTC) every day for a given site, setting the time difference threshold too small will result in a small number of matching stations (Fig. 1). Therefore, the time difference between the RS and Aeolus wind profiles is set within one hour. Note that 1 hour corresponds to an earth rotation of 15 degrees, i.e., a maximum distance to the Aeolus track of about 1500 km. Meanwhile, following the well-established geographical matching principle (Guo et al., 2020), the distance between an Aeolus wind profile and an RS site should be less than 75 km. After temporal and spatial collocation, the closest Aeolus wind profile to each RS profile is adopted for comparison.

In addition, it should be noted that RS has the problem of time and space drift in measuring the vertical wind profile (Baars et al., 2020; Martin et al., 2020). As shown in Fig. 3, there are some time and space differences between each pair of samples in collocating the profiles, due to the extended measurement cycle of a RS profile. Figs. 3a and 3b show, as an example, the distance and time difference between Aeolus and a RS wind profile, respectively. Although we use the start coordinates and start time of the RS to conduct the time and space matching with Aeolus data, the drift of a RS balloon may break these matching rules, especially at high altitude (above 15 km). It is not certain whether this drift will have a significant impact on the comparison results. Therefore, we analyse the impact of distance and time mismatches on the differences between Aeolus and RS wind speed, as shown in Fig. 4. Moreover, these data have also been screened for validity and estimated error thresholds. The blue and red boxes represent the Mie-cloudy and Rayleigh-clear winds, respectively. The text labels represent the mean of the differences between the Aeolus and RS HLOS wind speeds in the corresponding box. The box size shows the upper margin, upper quartile, median, lower quartile, lower margin of the difference in each bin. For Mie-cloudy winds (Figs. 4a and 4b), the difference between Mie-cloudy wind and RS winds is relatively constant with the distance and time differences increased. Similar to Mie-cloudy wind, the difference between Rayleigh-clear wind and RS wind is constant with the distance and time differences increased (Fig. 4c and 4d). These results indicate that the drift of the RS has rather small

https://doi.org/10.5194/amt-2022-26
Preprint. Discussion started: 26 January 2022

effect on the data that we use for comparison, the impact of RS drift can be excluded on subsequent comparisons.

2.4.2 Aeolus and ECMWF data

For the comparison of Aeolus and ECMWF data, the Aeolus L2C wind product contains the HLOS wind of ECMWF wind vector at each Aeolus bin. It means that we can obtain these two sets of data directly based on the Aeolus bin. The data for comparison is then filtered based on validity flag and the estimated errors. Note that the Aeolus L2C wind product is first published on 9 July 2020. Therefore, the matching period of Aeolus and ECMWF data is from 9 July 2020 to 30 September 2020.

2.4.3 RS and ERA5 data

In order to get more samples, the RS profile is directly matched with the gridded ERA5 data. The matching principle is to ensure that the time and space differences are minimized. Because of the daily launch time of RS twice per day at around 00:00 and 12:00 UTC, the gridded (0.25 x 0.25 degrees) ERA5 data at 00:00 and 12:00 UTC were downloaded. Meanwhile, according to the RS site coordinates, the ERA5 wind profile on the nearest grid position is obtained to match the RS wind profile. In the vertical direction, the ERA5 data has a total of 28 layers in the range of 0-20 km. For each layer, the data were matched with the closest sample point on the RS profile according to the pressure coordinates. Note that to be more compatible and comparable with the HLOS statistics, the RS winds are converted to zonal components to compare with ERA5 zonal components. In addition, the impact of RS drift on the difference between RS and ERA5 zonal wind components was also analysed as shown in Fig. S2. The wind difference (ERA5-RS) gradually grows with the distance, so does the time difference. This indicates that the RS drift may affect the comparison between RS and ERA5, resulting in a slightly higher RS zonal wind as compared to the ERA5 zonal wind.

https://doi.org/10.5194/amt-2022-26
Preprint. Discussion started: 26 January 2022


Atmospheric Measurement Techniques Discussions

2.5 Statistical method

For the Aeolus-ECMWF and RS-Aeolus comparison, the wind data were both converted to the Aeolus HLOS wind component. Only for the comparison of RS and ERA5 data, the wind data were converted to the zonal wind component. The wind component difference between wind component sample A and wind component sample B is given by:

$$v_{diff} = v_A - v_B \tag{2}$$

Moreover, the mean difference (MD) and standard deviation (SD) of v_{diff} for n samples are estimated according to:

$$\mathrm{MD} = \frac{1}{n}\sum_{i=1}^{n} v_{diff} \tag{3}$$

and

$$\mathrm{SD} = \sqrt{\frac{1}{n-1}\sum_{i=1}^{n}(v_{diff} - MD)^2} \tag{4}$$

The correlation coefficient (R) between wind component sample A and wind component sample B is calculated using:

$$\mathrm{R} = \frac{\sum_{i=1}^{n}(x_i-\bar{x})(y_i-\bar{y})}{\sqrt{\sum_{i=1}^{n}(x_i-\bar{x})^2}\sqrt{\sum_{i=1}^{n}(y_i-\bar{y})^2}} \tag{5}$$

where x_i and y_i represent the i-th sample point of A and B wind component dataset, respectively. $\bar{x}$ and $\bar{y}$ represent the mean wind component of the A and B wind component datasets, respectively.

3 Results and discussion

3.1 Overall intercomparison

The results of the comparison between Aeolus, RS and ERA5 (ECMWF) are shown in Fig. 5. The red and blue dots represent the Rayleigh-clear and Mie-cloudy winds, respectively. Figure 5a and 5d show that the Aeolus Rayleigh-clear and Mie-cloudy wind products over China are on average consistent

https://doi.org/10.5194/amt-2022-26
Preprint. Discussion started: 26 January 2022


Atmospheric Measurement Techniques Discussions

with RS wind observations. The mean difference of RS HLOS relative to Rayleigh-clear and Mie-cloudy HLOS are −0.24±7.01 and 0.18±4.42 m/s, respectively. Figure 5b and 5e illustrate the comparison between the Aeolus and ECMWF HLOS. The mean difference is −0.16±6.78 and −0.21±3.91 m/s for ECMWF winds relative to Rayleigh-clear and Mie-cloudy winds, respectively. As expected, since the HLOS observation data of Aeolus were assimilated in ECMWF operations, the wind values of Aeolus and ECMWF agree well. As a matter of fact, the comparison results between Aeolus and ECMWF winds depend (only) on the observation operator and expectations of 4D-var data assimilation. The 4D-var uses 3D spatial kernels for background (B) error representation, which spread the Aeolus observation (O) increments (O-B) in the ECMWF model domain. The kernels are based on the spread in an ensemble of forecasts and all observations in the temporal 4Dvar window (12 hours) are considered to produce an ECMWF model trajectory that is consistent with all observations. The analysis weight of the Aeolus observations O depends on the local ratio of the estimated background and observation error covariances. The Rayleigh-clear winds have (variable) estimated errors associated with them, but these are inflated before data assimilation in accordance with the estimated Aeolus Rayleigh errors. The Mie-cloudy winds are on the 10-km scale and can be closely spaced horizontally. ECMWF followed the arguments from Stoffelen et al. (2020) on observation density and spatial representativeness and found benefit in the forecasts by weight inflation of the Mie winds by a spatial representativeness error. In addition, the values of R and mean difference of RS vs ERA5 zonal winds are 0.97 and −0.46±3.12 m/s, respectively (Fig. 5c and 5f).

The spatial distributions of the correlation coefficients between the Aeolus, RS and ERA5 (ECMWF) wind speed data set are shown in Fig. 6. The comparison period for Aeolus vs RS is from 20 April to 30 September 2020, but for Aeolus vs ECMWF and RS vs ERA5 is from 9 July to 30 September 2020. In addition, the spatial distributions of the number of paired data samples are shown in Fig. S3. Figure 6a and 6b show the comparison results between Aeolus and RS HLOS winds. For Mie-cloudy winds, the correlation coefficients of most sites (51 out of 54, i.e., 94 %) are exceeding 0.8, lowest value (0.59)

https://doi.org/10.5194/amt-2022-26
Preprint. Discussion started: 26 January 2022


Atmospheric Measurement Techniques Discussions

are observed at Xinjiang. Similar to Mie-cloudy winds, also for the Rayleigh-clear winds, the R at most of the sites (50 out of 54, i.e., 93 %) is higher than 0.8, and the R values for the other four sites range from 0.7 to 0.8. As for the comparison result of Aeolus and ECMWF winds (Fig. 6c and 6d), we can see that the correlation between Rayleigh-clear (Mie-cloudy) and ECMWF winds along the ground track is very large. This result again indicates the consistency of Aeolus and ECMWF HLOS winds, mainly due to the assimilation of the Aeolus observation data. The similar results occur in the comparison results of zonal wind components between RS and ERA5 (Fig. 6e). The correlation between RS and ERA5 zonal wind components is very high (with R larger than 0.85) at all sites. Overall, the performance of Aeolus, RS and ERA5 wind products over China is similar to each other.

3.2 Vertical distribution of wind differences

The vertical distributions of the wind speed differences between Aeolus, RS and ERA5 (ECMWF) for ascending and descending orbits are shown in Fig. 7. The vertical distribution of the number of paired data samples is shown in Fig. S4. To ensure the validity of the statistics, we removed the paired data samples that were less than 20. For the comparison of Aeolus and RS HLOS data, the mean wind difference between the Mie-cloudy (Rayleigh-clear) and the RS winds is less than 2 m/s in the height range of 1−15 km during all observation times. During ascending and descending orbits, the vertical distributions of the HLOS differences are similar to that during all observation times. The maximum mean HLOS difference of the Mie-cloudy and Rayleigh-clear relative to RS winds during ascending (descending) orbits is −1.27±3.73 (-1.39±4.17) and 0.87±6.99 (−1.26±8.07) m/s, respectively. At the same time, it is noted that the wind speed difference between Rayleigh-clear and RS winds is mainly appeared in the height range of 2−3 km during the descending orbits. This is consistent with our previous validation work (Guo et al., 2020). Khaykin et al. (2020) also analyzed one wind profile of Aeolus with the Doppler lidar and found a good agreement between the two measurements, but below 5 km above ground level, a stronger deviation was observed, which was likely caused by horizontal

https://doi.org/10.5194/amt-2022-26
Preprint. Discussion started: 26 January 2022


Atmospheric Measurement Techniques Discussions

heterogeneity of the atmosphere. Moreover, Wu et al. (2021) compared the wind measurements in the atmospheric boundary layer with Aeolus and ground-based coherent Doppler lidar network over China, and pointed out that the vertical velocity could impact the HLOS wind velocity retrieval from Aeolus. Hence, considering the influence of turbulence and convection in the planetary boundary layers, the small difference between Rayleigh-clear and RS winds in the height range of 2−3 km may be due to the high vertical velocity during the descending orbits (12:00 UTC). For Aeolus and ECMWF data (Figs. 7d, 7e and 7f), due to the Aeolus assimilation at ECMWF, the HLOS difference between Aeolus and ECMWF along the vertical profile is small. There is no obvious deviation between Aeolus and ECMWF data. For the comparison of RS and ERA5 zonal wind components (Figs. 7g, 7h and 7i), the vertical distributions of the wind differences are similar during all time, ascending and descending orbits. The RS zonal winds are highly consistent with the ERA zonal winds in the height range of 1-13 km, and tend to be larger than ERA5 zonal winds above 13 km. As described in section 2.4.3, the difference between RS and ERA5 at high altitudes mainly caused by the RS drift. Overall, the three types of wind data have good consistency along the vertical profile.

3.3 Horizontal distribution of wind differences

To investigate the performance of Aeolus wind data in spatial distribution, the averaged value of Aeolus HLOS winds, RS zonal winds and ERA5 zonal winds during ascending and descending orbits are investigated from 9 July 2020 to 30 September 2020. The spatial distributions of the averaged value of Aeolus HLOS winds and RS zonal winds during ascending and descending orbits are presented in Fig. 8, where the ERA5 zonal wind data is used as the background values. The average HLOS result is only provided when the number of valid samples for Aeolus Rayleigh-clear and Mie-cloudy winds at each bin is larger than 10. The average wind is calculated from all valid winds on the Aeolus or RS profile during the corresponding observation period. During ascending orbits, the average winds of Rayleigh-clear and Mie-cloudy are similar to those of ERA5, with the average Rayleigh-clear HLOS wind is slightly higher in northwest China. The spatial distribution of average

https://doi.org/10.5194/amt-2022-26
Preprint. Discussion started: 26 January 2022


Atmospheric Measurement Techniques Discussions

zonal winds of RS follows a similar pattern as that of ERA5 (Fig. 8e). Similarly, during descending orbits, the spatial distributions of the average winds of Rayleigh-clear, Mie-cloudy and RS are similar to that of ERA5. These results indicated that the Aeolus HLOS winds have a good performance in China area. Previous study indicates that there are differences in bias between the ascending and descending orbit phase, which mainly occur for the Rayleigh channel in late summer and autumn (Martin et al., 2021). One reason is that the Aeolus field of view direction points to the right of the spacecraft into the dark side of the earth, implying that the viewing direction during the ascending (HLOS points east) and descending (HLOS points west) orbits are different. Another reason may be that the meteorological conditions such as wind speeds, BLH, air temperature and aerosol distributions during the ascending and descending orbits are different (Sun et al., 2014). However, in this study (Fig. S5 and S6), the mean differences between Rayleigh-clear (Mie-cloudy) winds and RS winds during the ascending and descending orbit phase are -0.07 ± 0.69 (-0.72 ± 1.48) and 0.3 ± 1.25 (0.1 ± 1.32) m/s. These small deviations (less than 0.8 m/s) indicate that the performance of Aeolus wind products may be unaffected by the orbit phase or HLOS wind conditions. Overall, the Aeolus HLOS winds are similar to the RS (ECMWF) winds during all observation times, and the mean differences for Mie-cloudy and Rayleigh-clear winds are -0.2 ± 1.32 (0.19 ± 0.89) and 0.19 ± 71 (0.13 ± 1.01) m/s, respectively (Fig. S7). The mean differences between RS and ERA5 zonal winds are 0.91 ± 0.35 m/s. These small differences are acceptable for application of wind products.

The comparison results obtained in this study, by and large, agree well with most of the validation work of Aeolus wind products, although the data sources and regions of interest vary a lot. For instance, Baars et al. (2020) revealed that the random errors were about 4 and 2.2 m/s for Rayleigh-clear and Mie-cloudy wind, respectively, by utilizing the RV Polarstern cruise from Bremerhaven to Cape Town. Lux et al. (2020) compared the Aeolus Rayleigh-clear wind observations to winds measured with the airborne demonstrator and the ECMWF model in central Europe. They reported a bias of 1.6 (2.53) m/s with random errors of 2.5 (3.57) m/s for the comparison against the ECMWF model (airborne

https://doi.org/10.5194/amt-2022-26
Preprint. Discussion started: 26 January 2022


Atmospheric Measurement Techniques Discussions

demonstrator). In a recent comparison analysis based on a combination of Aeolus, RS and numerical weather prediction model on a global scale, the mean absolute bias is found to be approximately 1.8–2.3 m/s for the Rayleigh winds and 1.3–1.9 m/s for the Mie winds (Martin et al., 2021).

4 Summary and conclusions

This study presents a comprehensive intercomparison analysis between the wind observations from Aeolus, ERA5 model winds and RS over China during the period 20 April 2020 to 30 September 2020. The correlation and difference between each set of data have been analysed to evaluate the Aeolus wind product characteristics. Furthermore, the spatial vertical and horizontal distributions of wind differences between each set of data have been investigated.

First, for the Aeolus and RS HLOS winds, the R and mean difference between the Rayleigh-clear (Mie-cloudy) and RS winds are 0.94 (0.97) and –0.24 ±7.01 (0.18 ±4.42) m/s, respectively. The vertical profiles of the HLOS differences are similar to each other during ascending and descending orbits. Moreover, for the Rayleigh-clear winds, the average HLOS differences are negative during ascending orbits (–0.07 ±0.69 m/s), whereas they are positive during descending orbits (0.3 ±1.25 m/s). These small deviations indicate that the performance of Aeolus wind products may be unaffected by the orbit phase or HLOS wind conditions. For the Aeolus and ECMWF winds, as expected, due to assimilation of the Aeolus wind products in the ECMWF model, the wind results of Aeolus and ECMWF show good consistency spatially. The R and mean difference of Rayleigh-clear and Mie-cloudy HLOS winds relative to ECMWF winds are 0.95 (0.97) and –0.16 ±6.78 (–0.21 ±3.91) m/s, respectively. The correlation and difference between Aeolus and ECMWF winds mainly depend on the data assimilation settings. In addition, a small difference between Rayleigh-clear winds relative to RS winds is appeared in the height range of 2−3 km during descending orbits. This result may be due to the high vertical velocity during the descending orbits (12:00 UTC). For the RS and ERA5 zonal winds, the mean

https://doi.org/10.5194/amt-2022-26
Preprint. Discussion started: 26 January 2022


Atmospheric Measurement Techniques Discussions

difference and R of ERA5 and RS zonal winds are −0.46±3.12 m/s and 0.97, respectively. Along the vertical, the wind speed differences are very small in the height range of 0-13 km and positive in the height range of 13-16 km. The difference between RS and ERA5 at high altitudes mainly caused by the RS drift. Overall, the Aeolus HLOS winds, RS zonal winds and ERA5 zonal winds are similar to each other during all observation times.

Our work comprehensively compares the wind products form Aeolus, RS and ERA5 (ECMWF) over large regional spatial scales in mainland China. From the perspective of correlation and magnitude of difference between samples, we conclude that the winds form Aeolus, RS and ERA5 (ECMWF) are similar to each other. Some profile biases warrant further investigation however. The information collected is helpful to improve our confidence of applying Aeolus wind products in numerical weather prediction over China and in research on climate change.

Data availability

The L-band radiosonde data used in this paper can be provided for non-commercial research purposes upon request (Dr. Jianping Guo: jpguocams@gmail.com). The Aeolus dataset can be downloaded from https://aeolus-ds.eo.esa.int/oads/access/collection (last accessed 24 October 2020). Instructions for use and data access methods can be found on the official website. The ERA5 wind data can be download from https://cds.climate.copernicus.eu/cdsapp#!/dataset/reanalysis-era5-pressure-levels?tab=form.

Author contributions

The study was completed with close cooperation between all authors. J. Guo and B. Liu conceived of the idea for assessing the Aeolus wind products using radiosonde measurements in China; J. Guo and B. Liu conducted the data analyses and co-wrote the manuscript; Y. Ma, W. Gong, A. Stoffelen, G. Leeuw, and X. Xu discussed the experimental results, and all coauthors helped reviewing the manuscript.

Competing interests.

The authors declare that they have no conflict of interest.

Special issue statement.

This article is part of the special issue "Aeolus data and their application". It is not associated with a conference.

Acknowledgements.

We are very grateful to the China Meteorological Administration for the operation and maintenance of the radiosonde observational network, to ESA for the Aeolus data and to ECMWF for ERA5. This work was financially supported by the National Natural Science Foundation of China under grants 42001291, 91637211 and 41771399. The study contributes to the ESA/MOST cooperation project DRAGON5, Topic 3 Atmosphere, sub-topic 3.2 Air-Quality and the ESA Aeolus DISC project.

References

Albertema, S.: Validation of Aeolus satellite wind observations with aircraft-derived wind data and the ECMWF NWP model for an enhanced understanding of atmospheric dynamics, Master thesis Utrecht Un., the Netherlands, 2019 (https://dspace.library.uu.nl/handle/1874/383392).

Benjamin, S. G., Schwartz, B. E., Szoke, E. J., and Koch, S. E.: The value of wind profiler data in US weather forecasting. Bulletin of the American Meteorological Society, 85(12), 1871-1886, 2004.

Baars, H., Herzog, A., Heese, B., Ohneiser, K., Hanbuch, K., Hofer, J., Yin, Z., Engelmann, R., and Wandinger, U.: Validation of Aeolus wind products above the Atlantic Ocean, Atmos. Meas. Tech., 13, 6007–6024, https://doi.org/10.5194/amt-13-6007-2020, 2020.

Belmonte Rivas, M. and Stoffelen, A.: Characterizing ERA-Interim and ERA5 surface wind biases using ASCAT, Ocean Sci., 15, 831–852, https://doi.org/10.5194/os-15-831-2019, 2019.

https://doi.org/10.5194/amt-2022-26
Preprint. Discussion started: 26 January 2022


Atmospheric Measurement Techniques Discussions

Constantinescu, E.M., Zavala, V.M., Rocklin, M., Lee, S., and Anitescu, M.: Unit commitment with wind power generation: integrating wind forecast uncertainty and stochastic programming (No. ANL/MCS-TM-309). Argonne National Lab. (ANL), Argonne, IL, United States, 2009.

Dabas, A., Denneulin, M.L., Flamant, P., Loth, C., Garnier, A. and Dolfi-Bouteyre, A.: Correcting winds measured with a Rayleigh Doppler lidar from pressure and temperature effects, Tellus A 60, 206-215. doi:10.1111/j.1600-0870.2007.00284.x. 2008.

De Kloe, J., Stoffelen, A., Tan, D., Andersson, E., Rennie, M., Dabas, A., Poli, P., and Huber, D.: ADM-Aeolus Level-2B/2C Processor Input/Output Data Definitions Interface Control Document, Tech. rep., AE-IF-ECMWF-L2BP-001, v. 3.0, 100 pp., 2017.

European Space Agency (ESA): "ADM-Aeolus Science Report," ESA SP-1311, 121 p., http://esamultimedia.esa.int/docs/SP-1311_ADM-Aeolus_FINAL_low-res.pdf, 2008.

European Space Agency (ESA): "ADM-Aeolus Mission Requirements Document", ESA EOP-SM/2047, 57 p., http://esamultimedia.esa.int/docs/EarthObservation/ADM-Aeolus_MRD.pdf, 2016.

Fan J., M. Ovtchinnikov, J.M. Comstock, S.A. McFarlane, and A. Khain: Ice Formation in Arctic Mixed-Phase Clouds: Insights from a 3-D Cloud-Resolving Model with Size-Resolved Aerosol and Cloud Microphysics. J. Geophys. Res. Atmos., 114, D04205, doi:10.1029/2008JD010782, 2009.

Guo, J., Miao, Y., Zhang, Y., Liu, H., Li, Z., Zhang, W., He, J., Lou, M., Yan, Y., Bian, L., and Zhai, P.: The climatology of planetary boundary layer height in China derived from radiosonde and reanalysis data. Atmos. Chem. Phys. 16, 13309, doi:10.5194/acp-16-13309-2016, 2016.

Guo, J., Su, T., Li, Z., Miao, Y., Li, J., Liu, H., Xu, H., Cribb, M., and Zhai, P.: Declining frequency of summertime local-scale precipitation over eastern China from 1970–2010 and its potential link to aerosols, Geophysical Research Letters, 44, 5700–5708, doi:10.1002/2017GL073533, 2017.

Guo, J., Liu, H., Li, Z., Rosenfeld, D., Jiang, M., Xu, W., Jiang, J. H., He, J., Chen, D., Min, M., and Zhai, P.: Aerosol-induced changes in the vertical structure of precipitation: a perspective of TRMM precipitation radar. Atmos. Chem. Phys., 18, 13329–13343, doi:10.5194/acp-18-13329-2018, 2018.

Guo, J., Y. Li, J. Cohen, J. Li, D. Chen, H. Xu, L. Liu, J. Yin, K. Hu, P. Zhai: Shift in the temporal trend of boundary layer height trend in China using long-term (1979–2016) radiosonde data. Geophysical Research Letters, 46 (11): 6080-6089, doi: 10.1029/2019GL082666, 2019.

Guo, J., Liu, B., Gong, W., Shi, L., Zhang, Y., Ma, Y., Zhang, J., Chen, T., Bai, K., Stoffelen, A., de Leeuw, G., and Xu, X.: Technical Note: First comparison of wind observations from ESA's satellite mission Aeolus and ground-based Radar wind profiler network of China, Atmos. Chem. Phys. Discuss., https://doi.org/10.5194/acp-2020-869, in review, 2020.

Houchi, K., Stoffelen, A., Marseille, G. J., and De Kloe, J.: Comparison of wind and wind shear climatologies derived from high-resolution radiosondes and the ECMWF model, *J. Geophys. Res.*, 115, D22123, doi:10.1029/2009JD013196, 2010.

Hoffmann, L., Günther, G., Li, D., Stein, O., Wu, X., Griessbach, S., Heng, Y., Konopka, P., Müller, R., Vogel, B., and Wright, J. S.: From ERA-Interim to ERA5: the considerable impact of ECMWF's next-generation reanalysis on Lagrangian transport simulations. Atmos. Chem. Phys., 19, 3097–3124, https://doi.org/10.5194/acp-19-3097-2019, 2019.

Hersbach, H., Bell, B., Berrisford, P., et al.: The ERA5 global reanalysis. Quarterly Journal of the Royal Meteorological Society, https://doi.org/10.1002/qj.3803, 2020.

Kanitz, T., Witschas, B., Marksteiner, U., Flament, T., Rennie, M., Schillinger, M., Parrinello, T., Wernham, D., and Reitebuch, O.: ESA's Wind Lidar Mission Aeolus – Instrument Performance and Stability, EGU General Assembly 2020, Online, 4–8 May 2020, EGU2020-7146, 2020, https://doi.org/10.5194/egusphere-egu2020-7146.

https://doi.org/10.5194/amt-2022-26
Preprint. Discussion started: 26 January 2022


Atmospheric Measurement Techniques Discussions

Koren, I., Kaufman, Y.J., Rosenfeld, D., Remer, L.A., and Rudich, Y.: Aerosol invigoration and restructuring of Atlantic convective clouds. Geophys. Res. Lett., 32, L14828, doi:10.1029/2005GL023187, 2005.

Khaykin, S. M., Hauchecorne, A., Wing, R., Keckhut, P., Godin-Beekmann, S., Porteneuve, J., Mariscal, J.-F., and Schmitt, J.: Doppler lidar at Observatoire de Haute-Provence for wind profiling up to 75 km altitude: performance evaluation and observations, Atmos. Meas. Tech., 13, 1501–1516, https://doi.org/10.5194/amt-13-1501-2020, 2020.

Li, Z., Niu, F., Fan, J., Liu, Y., Rosenfeld, D., and Ding, Y.: Long-term impacts of aerosols on the vertical development of clouds and precipitation. Nature Geoscience, 4(12), 888-894, 2011.

Liu, B., Ma, Y., Gong, W., Zhang, M., and Yang, J.: Study of continuous air pollution in winter over Wuhan based on ground-based and satellite observations. Atmospheric Pollution Research, 9(1), 156-165, 2018.

Liu, B., Ma, Y., Guo, J., Gong, W., Zhang, Y., Mao, F., Li, J., Guo, X., and Shi, Y.: Boundary layer heights as derived from ground-based Radar wind profiler in Beijing. IEEE Trans. Geosci. Remote Sens., 57 (10), 8095–8104. doi: 10.1109/TGRS.2019.2918301, 2019.

Liu, B., Guo, J., Gong, W., Shi, Y., and Jin, S.: Boundary layer height as estimated from Radar wind profilers in four cities in China: Relative contributions from Aerosols and surface features. Remote Sens., 12(10), 1657, 2020a.

Liu, B., Guo, J., Gong, W., Shi, L., Zhang, Y., and Ma, Y.: Characteristics and performance of vertical winds as observed by the radar wind profiler network of China. Atmos. Meas. Tech., doi:10.5194/amt-2020-75, 2020b.

Lux, O., Lemmerz, C., Weiler, F., Marksteiner, U., Witschas, B., Rahm, S., Schäfler, A., and Reitebuch, O.: Airborne wind lidar observations over the North Atlantic in 2016 for the pre-launch validation

https://doi.org/10.5194/amt-2022-26
Preprint. Discussion started: 26 January 2022

Atmospheric Measurement Techniques Discussions

of the satellite mission Aeolus. Atmos. Meas. Tech., 11, 3297–3322, doi:10.5194/amt-11-3297-2018, 2018

Lux, O., Lemmerz, C., Weiler, F., Marksteiner, U., Witschas, B., Rahm, S., Geiß, A., and Reitebuch, O.: Intercomparison of wind observations from the European Space Agency's Aeolus satellite mission and the ALADIN Airborne Demonstrator. Atmos. Meas. Tech., 13(4), 2020.

Marksteiner, U., Lemmerz, C., Lux, O., Rahm, S., Schäfler, A., Witschas, B., and Reitebuch, O.: Calibrations and Wind Observations of an Airborne Direct-Detection Wind LiDAR Supporting ESA's Aeolus Mission, Remote Sensing, 10, 2056, https://doi.org/10.3390/rs10122056, 2018.

Martin, A., Weissmann, M., Reitebuch, O., Rennie, M., Geiß, A., and Cress, A.: Validation of Aeolus winds using radiosonde observations and numerical weather prediction model equivalents, Atmos. Meas. Tech., 14, 2167–2183, https://doi.org/10.5194/amt-14-2167-2021, 2021.

Pu, Z., Zhang, L., and Emmitt, G. D.: Impact of airborne Doppler wind lidar profiles on numerical simulations of a tropical cyclone, Geophys. Res. Lett., 37, L05801, doi:10.1029/2009GL041765, 2010.

Reitebuch, O.: The Spaceborne Wind Lidar Mission ADM-Aeolus, in: Atmospheric Physics, edited by: Schumann, U., Springer Berlin, Heidelberg, 487–507, 2012.

Rennie, M. P. and Isaksen, L.: An Assessment of the Impact of Aeolus Doppler Wind Lidar Observations for Use in Numerical Weather Prediction at ECMWF, EGU General Assembly 2020, Online, 4–8 May 2020, EGU2020-5340, https://doi.org/10.5194/egusphere-egu2020-5340, 2020.

Rennie, M. P.: An assessment of the expected quality of Aeolus Level-2B wind products, EPJ Web Conf., 176, 02015, https://doi.org/10.1051/epjconf/201817602015, 2018.

https://doi.org/10.5194/amt-2022-26
Preprint. Discussion started: 26 January 2022


Atmospheric Measurement Techniques Discussions

Shi, Y., Liu, B., Chen, S., Gong, W., Ma, Y., Zhang, M. et al.: Characteristics of aerosol within the nocturnal residual layer and its effects on surface $PM_{2.5}$ over China. Atmos. Environ., 241, 117841, 2020.

Simonin, D., Ballard, S. P., and Li, Z. Doppler radar radial wind assimilation using an hourly cycling 3D-Var with a 1.5 km resolution version of the Met Office Unified Model for nowcasting. Quarterly Journal of the Royal Meteorological Society, 140(684), 2298-2314, 2014.

Stettner, D., Velden, C., Rabin, R., Wanzong, S., Daniels, J., and Bresky, W.: Development of enhanced vortex-scale atmospheric motion vectors for hurricane applications. Remote Sens., 11(17), 1981, 2019.

Stoffelen, A., A. Benedetti, R. Borde, A. Dabas, P. Flamant, M. Forsythe, M. Hardesty, L. Isaksen, E. Källén, H. Körnich, T. Lee, O. Reitebuch, M. Rennie, L. Riishøjgaard, H. Schyberg, A. G. Straume, and : Wind profile satellite observation requirements and capabilities. Bull. Amer. Meteor. Soc., https://doi.org/10.1175/BAMS-D-18-0202.1, 2020.

Stoffelen, A., Vogelzang, J., Marseille, G.-J.: High Resolution data assimilation guide. EUMETSAT NWP SAF Documentation, version 1.3, available: https://nwp-saf.eumetsat.int/site/download/documentation/scatterometer/reports/High_Resolution_Wind_Data_Assimilation_Guide_1.3.pdf, 2020.

Stoffelen, A., Pailleux, J., Källén, E., Vaughan, J. M., Isaksen, L., Flamant, P., Wergen, W., Andersson, E., Schyberg, H., Culoma, A., Meynart, R., Endemann, M., and Ingmann, P.: The atmospheric dynamics mission for global wind field measurement. B. Am. Meteorol. Soc., 86, 73–88, 2005.

Sun, X. J., Zhang, R. W., Marseille, G. J., Stoffelen, A., Donovan, D., Liu, L., and Zhao, J.: The performance of Aeolus in heterogeneous atmospheric conditions using high-resolution radiosonde data, Atmos. Meas. Tech., 7, 2695–2717, https://doi.org/10.5194/amt-7-2695-2014, 2014.

https://doi.org/10.5194/amt-2022-26
Preprint. Discussion started: 26 January 2022

Atmospheric Measurement Techniques Discussions

Su, T., Li, Z., Zheng, Y., Luan, Q., and Guo, J.: Abnormally shallow boundary layer associated with severe air pollution during the COVID-19 lockdown in China. Geophys. Res. Lett., 47, e2020GL090041. https://doi.org/10.1029/2020GL090041, 2020.

Tan, D. G. H., Andersson, E., de Kloe, J., Marseille, G., Stoffelen, A., Poli, P., Denneulin, M., Dabas, A., Huber, D., Reitebuch, O., Flamant, P., Le Rille, O., and Nett, H.: The ADM-Aeolus wind retrieval algorithms. Tellus A, 60, 191–205, 2008.

Tan, D., Rennie, M., Andersson, E., Poli, P., Dabas, A., de Kloe, J., Marseille, G.-J., and Stoffelen, A.: Aeolus Level-2B Algorithm Theoretical Basis Document, Tech. rep., AE-TN-ECMWFL2BP-0023, v. 3.0, 109 pp., 2017.

Witschas, B., Lemmerz, C., Geiß, A., Lux, O., Marksteiner, U., Rahm, S., Reitebuch, O., and Weiler, F.: First validation of Aeolus wind observations by airborne Doppler wind lidar measurements. Atmospheric Measurement Techniques, 13(5), 2381–2396, 2020.

Wu, S., Sun, K., Dai, G., Wang, X., Liu, X., Liu, B., Song, X., Reitebuch, O., Li, R., Yin, J., and Wang, X.: Inter-comparison of wind measurements in the atmospheric boundary layer with Aeolus and a ground-based coherent Doppler lidar network over China, Atmos. Meas. Tech. Discuss. [preprint], https://doi.org/10.5194/amt-2021-260, in review, 2021.

Yang Y., Yim S.H.L., Haywood J., Osborne M., Chan J.C.S., Zeng Z., Cheng J.C.H.: Characteristics of heavy particulate matter pollution events over Hong Kong and their relationships with vertical wind profiles using high-time-resolution Doppler Lidar measurements. Journal of Geophysical Research - Atmospheres, 124(16), 9609-9623, 2019.

Zhang, Y., J. Guo, Y. Yang, Y. Wang, and S.H.L. Yim: Vertical wind shear modulates particulate matter pollutions: A perspective from Radar wind profiler observations in Beijing, China. Remote Sensing, 12(3), 546. https://doi.org/10.3390/rs12030546, 2020.

https://doi.org/10.5194/amt-2022-26
Preprint. Discussion started: 26 January 2022

Atmospheric Measurement Techniques Discussions

Figures:

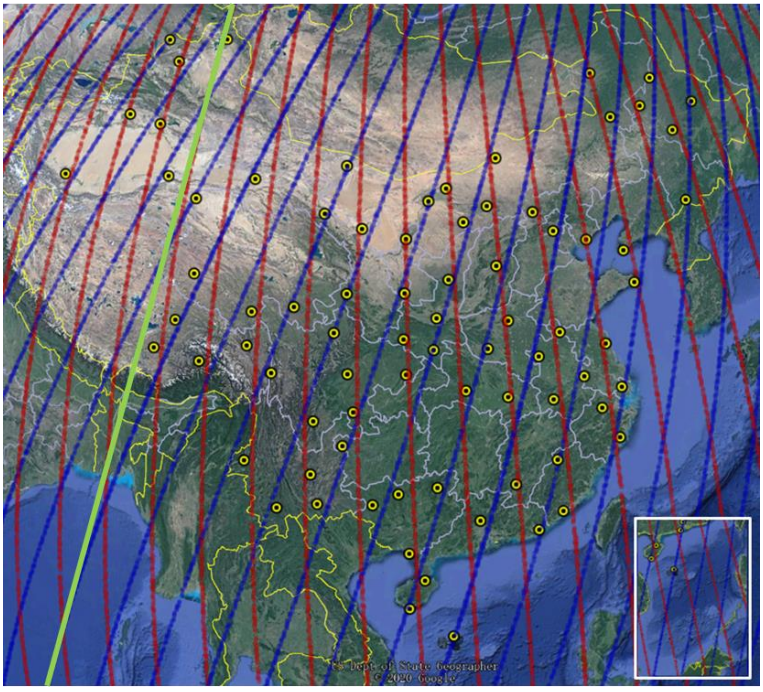

Figure 1. Geographic distribution of RS sites and Aeolus ground tracks superimposed on the GoogleEarth map of China (© Google Maps). Red and blue lines represent the Aeolus ground tracks for ascending and descending orbits, respectively. The yellow dots denote the RS sites. The green line approximates 90E, which is the approximate position of Aeolus at 12:00 and 0:00 UTC, the launch times of the radiosondes. Eastern RS are taken about 2.5 hours after Aeolus overpass time.

https://doi.org/10.5194/amt-2022-26
Preprint. Discussion started: 26 January 2022

Atmospheric Measurement Techniques Discussions

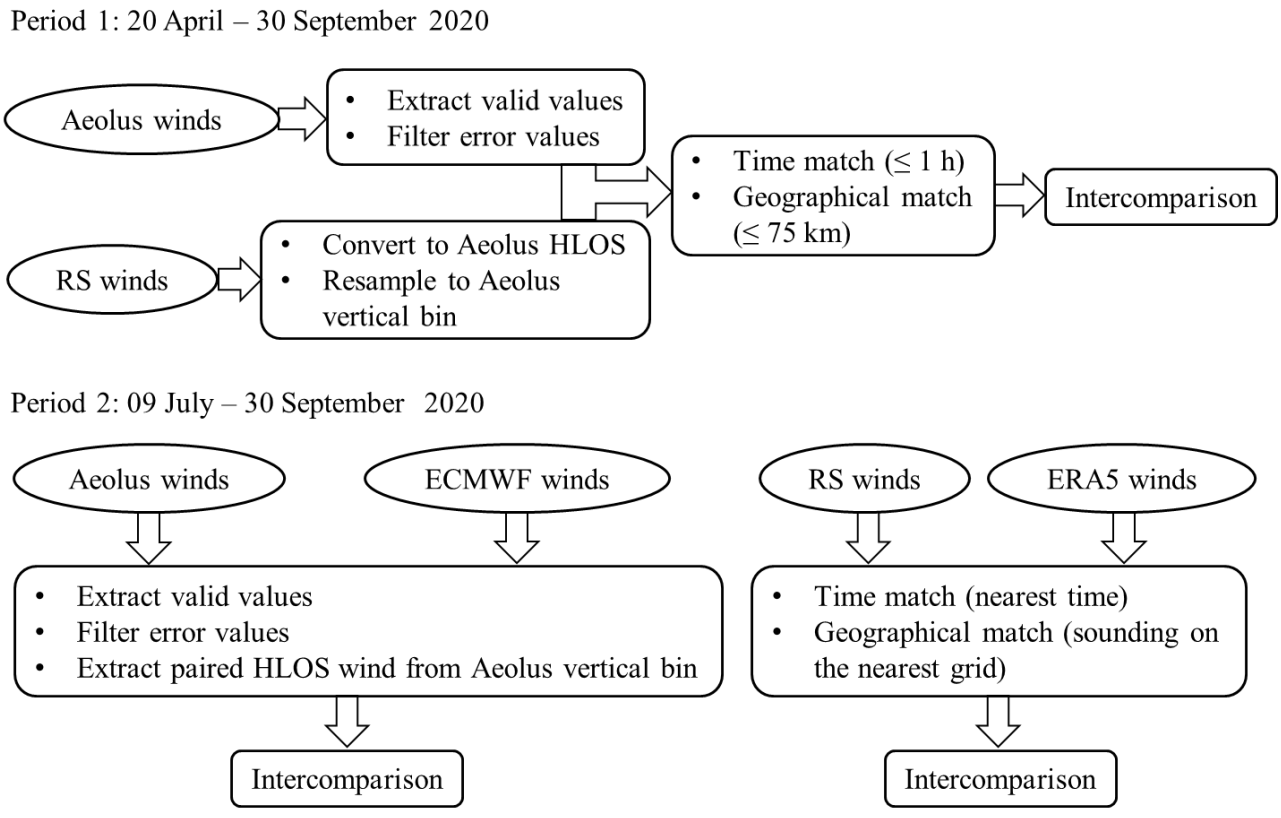

Figure 2. Flowchart showing the main processing procedures used to compare the wind observations from Aeolus, RS and ERA5 (ECMWF).

5

https://doi.org/10.5194/amt-2022-26
Preprint. Discussion started: 26 January 2022

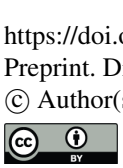

Atmospheric Measurement Techniques Discussions

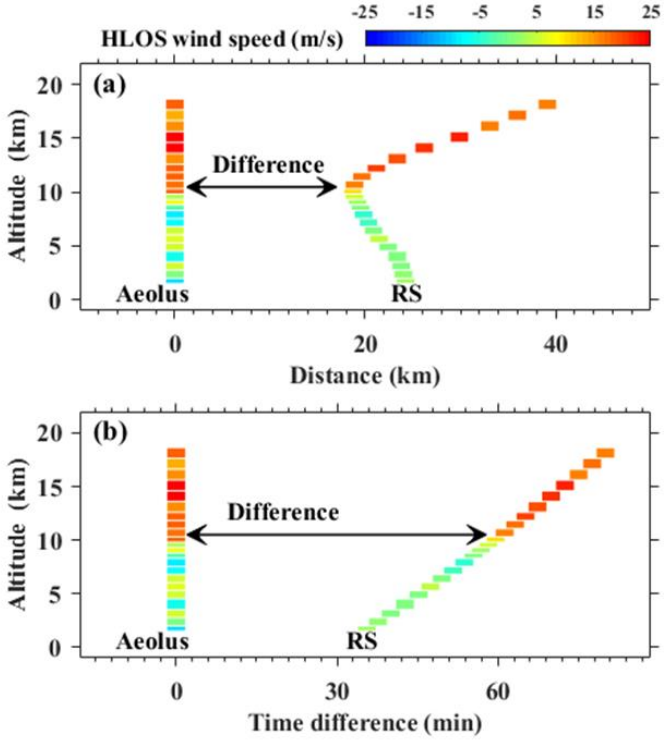

Figure 3. The examples on 24 Apr 2020 illustrating how the Aeolus HLOS profile is matched with RS HLOS profile in terms of (a) distance and (b) time difference between paired samples, which is based on the collocated time and space of Aeolus sampling grid as described in the text.

5

https://doi.org/10.5194/amt-2022-26
Preprint. Discussion started: 26 January 2022

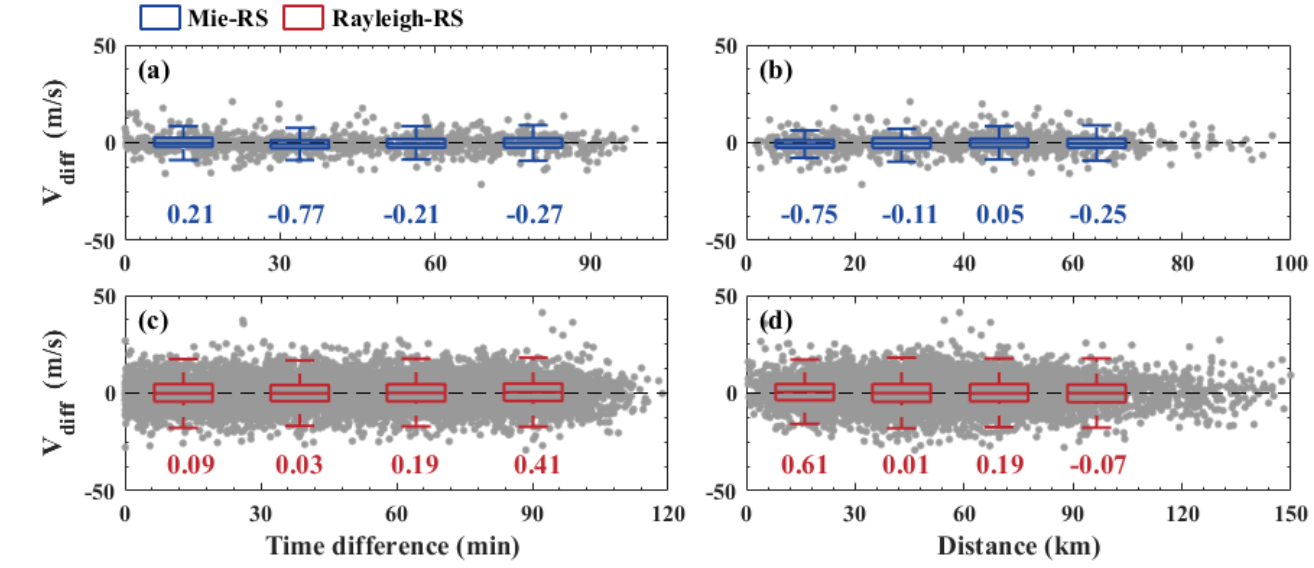

Figure 4. Difference between the Aeolus and RS HLOS as a function of (a, c) time difference and (b, d) distance. Blue, red box and gray dots indicate the Mie-cloudy, Rayleigh-clear winds and the corresponding sample points, respectively. The text labels represent the mean difference of the differences between Aeolus vs RS for each individual bin. The box size shows the upper margin, upper quartile, median, lower quartile, lower margin of the difference in each bin.

https://doi.org/10.5194/amt-2022-26
Preprint. Discussion started: 26 January 2022

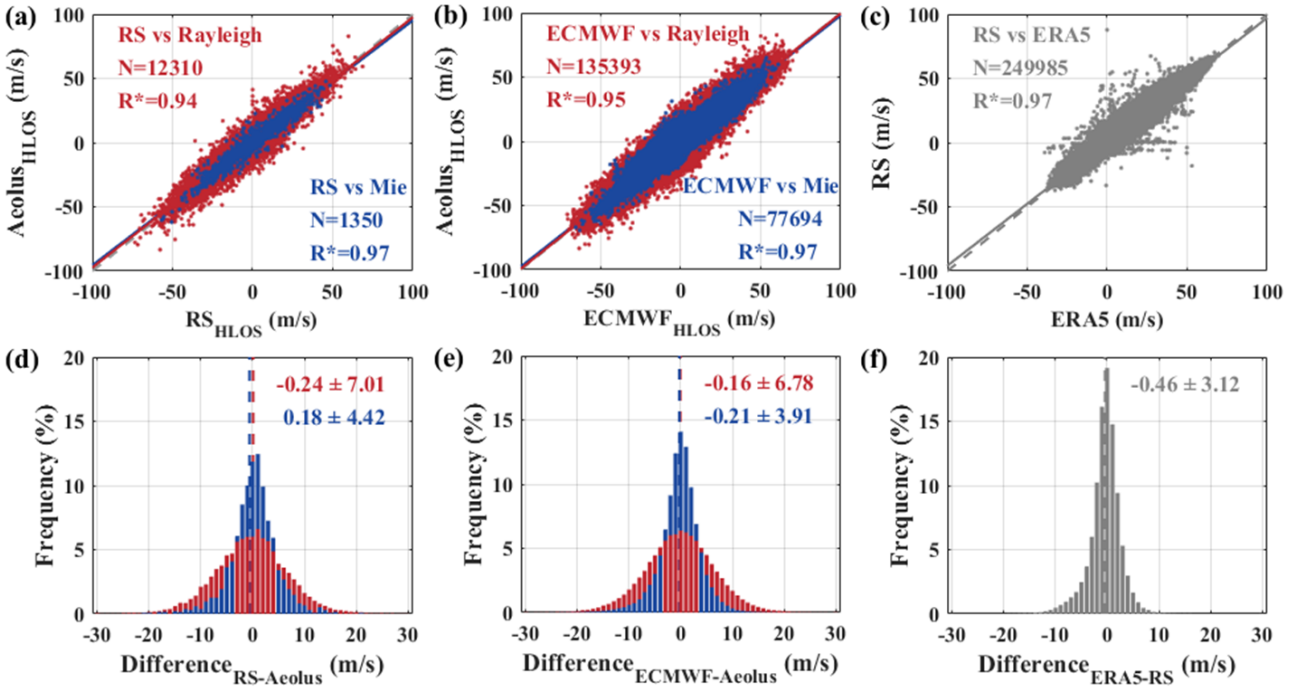

Figure 5. Scatterplots and histograms for (a, d) RS and Aeolus HLOS winds, (b,e) ECMWF and Aeolus HLOS winds and (c,f) ERA5-RS zonal wind components comparison results. Corresponding least-square line fits are indicated by the solid lines. The fit results are shown in the insets. The histogram plots show the mean and standard deviation in the insets. Blue and red indicate the Mie-cloudy and Rayleigh-clear winds, respectively. The 1:1 line is represented by the gray dashed line.

https://doi.org/10.5194/amt-2022-26
Preprint. Discussion started: 26 January 2022

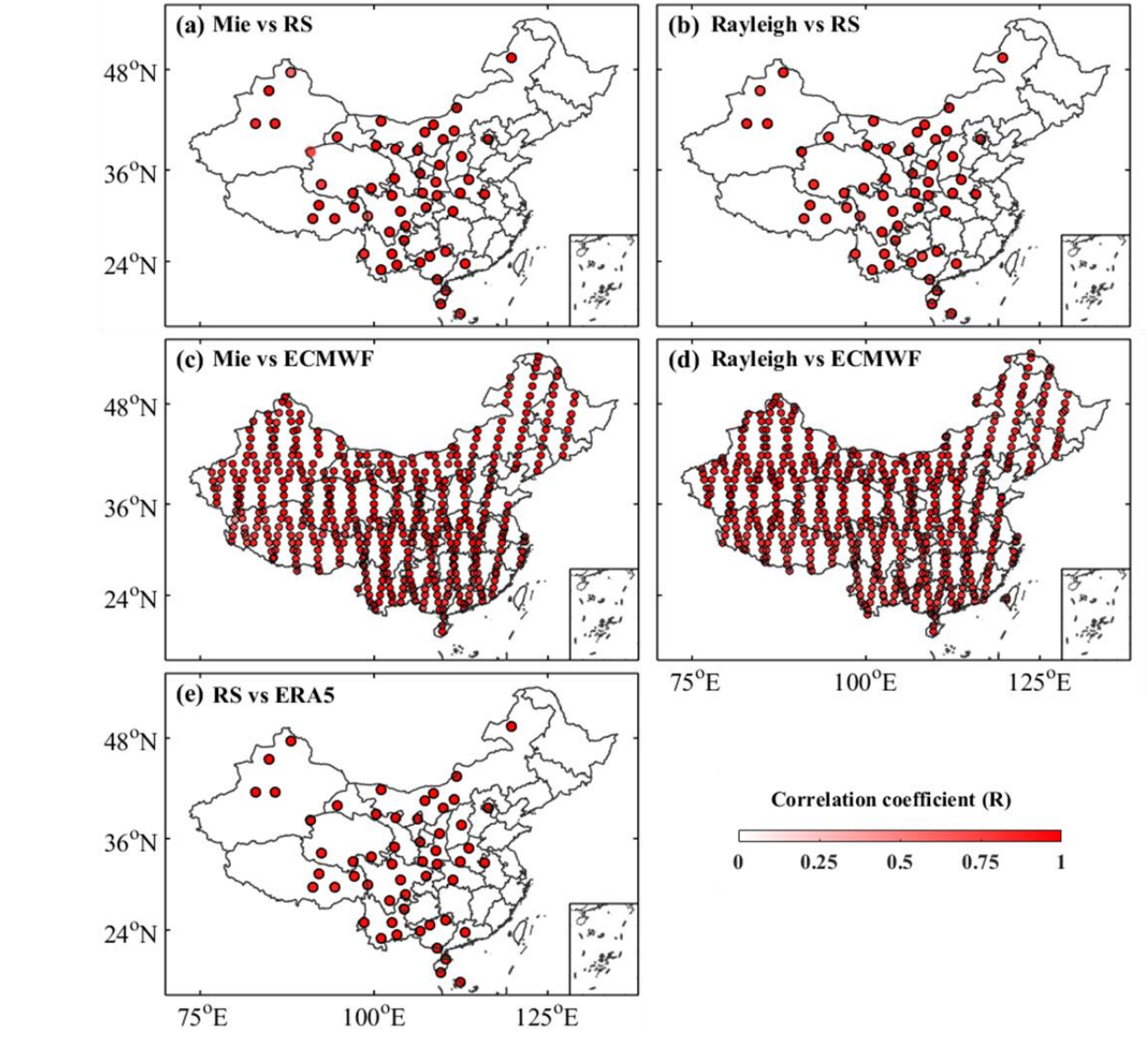

Figure 6. Geographic distribution of correlation coefficients between (a) Mie and RS, (b) Rayleigh and RS, (c) Mie and ECMWF, (d) Rayleigh and ECMWF and (e) RS and ERA5 winds. Note that the comparison period for Aeolus vs RS is from 20 April to 30 September 2020, but for Aeolus vs ECMWF and RS vs ERA5 is from 9 July to 30 September 2020. The black circles indicate the RS sites where the correlation coefficients between each data pair passed the statistic significance test ($P<0.05$).

https://doi.org/10.5194/amt-2022-26
Preprint. Discussion started: 26 January 2022

Atmospheric Measurement Techniques Discussions

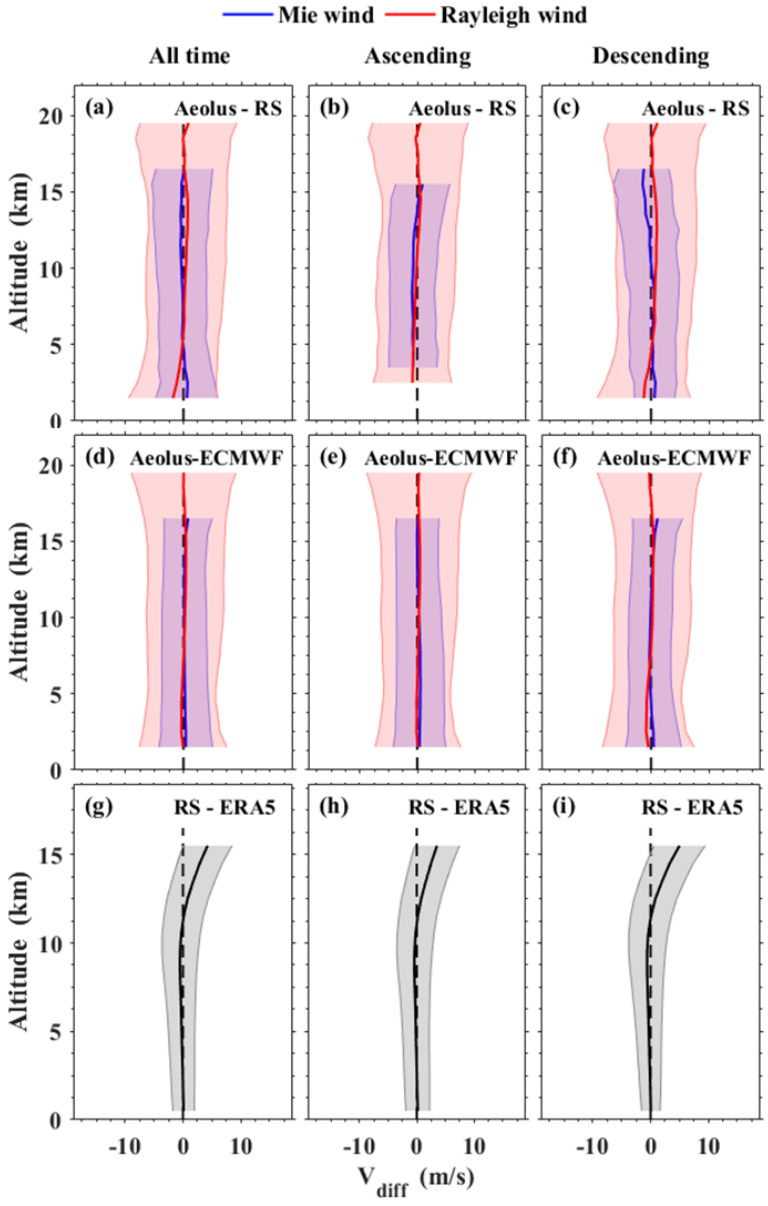

Figure 7. Vertical distributions of the wind HLOS difference between Aeolus, RS and ECMWF for (a, d) all time, (b, e) ascending, and (c, f) descending orbits and similar for RS and ERA5 zonal wind components at the different categories (resp. g, h and i). The altitude is above sea level.

https://doi.org/10.5194/amt-2022-26
Preprint. Discussion started: 26 January 2022

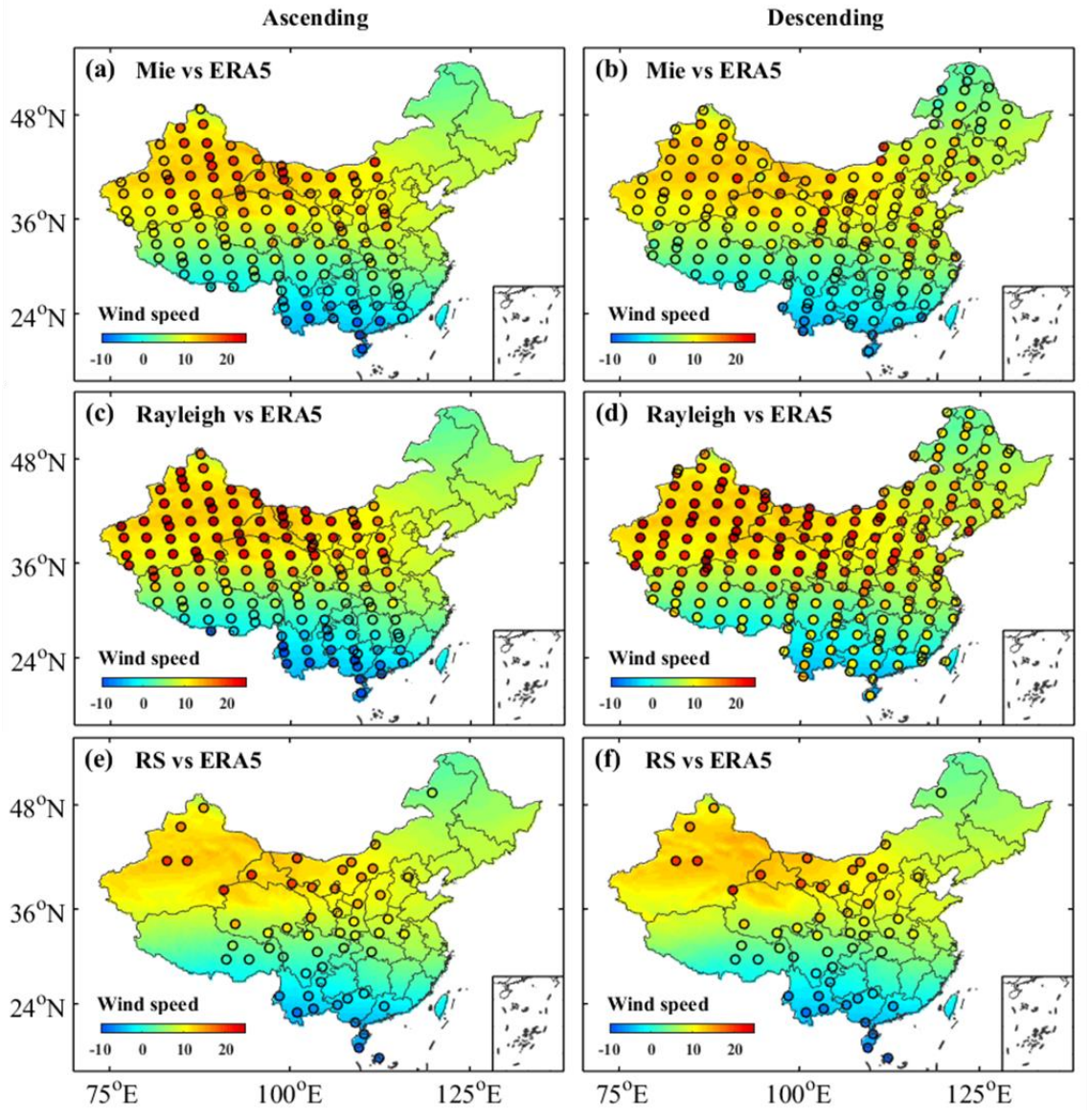

Figure 8. The average value of Aeolus HLOS wind and RS zonal wind components during (a, c, e) ascending and (b, d, f) descending orbits from 9 July 2020 to 30 September 2020. The color circles represent the average value of corresponding Aeolus HLOS wind or the RS zonal wind components. The ERA5 zonal wind component data (color shading) are shown as the background values.